

Supporting Information

Enhancing Solar-Thermal-Electric Energy Conversion Based on m-PEGMA/GO Synergistic Phase Change Aerogels

Ruirui Cao^{1,2*}, Dequan Sun³, Liangliang Wang¹, Zhengguang Yan¹, Wenquan Liu¹,
Xin Wang^{1*}, and Xingxiang Zhang^{2,4*}

¹Henan Key Laboratory of Photovoltaic Materials, Henan University, Kaifeng 475004, China

²School of Material Science and Engineering, Tiangong University, Tianjin 300387, China

³Xinlian College of Henan Normal University, Zhengzhou 450046, China

⁴Tianjin Municipal Key Lab of Advanced Fiber and Energy Storage Technology, Tianjin 300387, China

Corresponding Author

* Ruirui Cao, E-mail: rrcao0403@vip.henu.edu.cn

* Xin Wang, E-mail: xwang2008@vip.henu.edu.cn

* Xingxiang Zhang, E-mail: zhangpolyu@aliyun.com

Characterization

Fourier-transformed infrared (FT-IR) spectra were recorded on a spectrometer (VERTEX 70, Bruker, Germany) in the range of 4000 to 400 cm^{-1} . Raman spectra were recorded on an XploRA PLUS Raman microscope (Horiba Company, Japan) equipped with a 638-nm laser source. The morphology and microscopic structure of PCAs were characterized by field-emission SEM system (Gemini SEM500, ZEISS Company, Germany) with an accelerating voltage of 10 kV. X-ray diffraction (XRD) was performed using a Rigaku D/MAX-gA diffractometer (Rigaku Company, Japan) with a filtered Cu $K\alpha$ radiation source ($\lambda = 0.15406$ nm). Diffractograms were obtained in the range of 3° to 40° (2θ) and a scan rate of $8^\circ/\text{min}$. The thermal property of PCAs were evaluated by differential scanning calorimetry (DSC, DSC200 F3, NETZSCH Company, Germany) in the range of $-10\sim 100^\circ\text{C}$ at a rate of $\pm 10^\circ\text{C}/\text{min}$ under a nitrogen atmosphere. Thermogravimetric analysis (TGA) was evaluated on a thermogravimetric analyzer (STA449F3, NETZSCH Company, Germany) in the range of $40\sim 800^\circ\text{C}$ at a heating rate of $10^\circ\text{C}/\text{min}$ under a nitrogen atmosphere. The thermal reliability of 100 heating/cooling cycles was measured by a programmable controller (Giant Force, China) with temperature changing from 0 to 80°C . After that, the thermal reliability and structural stability were determined by DSC and FT-IR analysis, respectively, before and after 100 thermal cycles. Solar-thermal-electric energy conversion and storage of PCA-loaded TEGs were characterized by a handy thermometer (RKC Instrument Inc., Japan), a simulated solar illumination (CEL-S500/350, CEAULIGHT, China) at a constant intensity of $200\text{ mW}/\text{cm}^2$, and a Keithley electrometer (6514 System Electrometer, A Tektronix Company).¹ Therein, the PCA3 (4.50 g) and PCA4 (2.75 g) were encapsulated on the side of commercial thermoelectric device to fabricate PCA-loaded TEGs, which were marked as TEG1 and TEG2, respectively. The thermoelectric figure of merit (ZT) of the commercial thermoelectric device used in this study is about $0.75\sim 0.9$.

Table S1. Experimental parameters.

Specimen	m-PEGMA (g)	APS (g)	GO (wt%) ^a	EDA (μL)
c-PCM	5.0	0.05	0.0	0
PCA1	5.0	0.05	0.5	40
PCA2	5.0	0.05	1.0	80
PCA3	5.0	0.05	1.5	120
PCA4	5.0	0.05	2.0	160
PCA5	5.0	0.05	3.0	240
PCA6	5.0	0.05	5.0	400

^a The loading of GO in the experimental section.

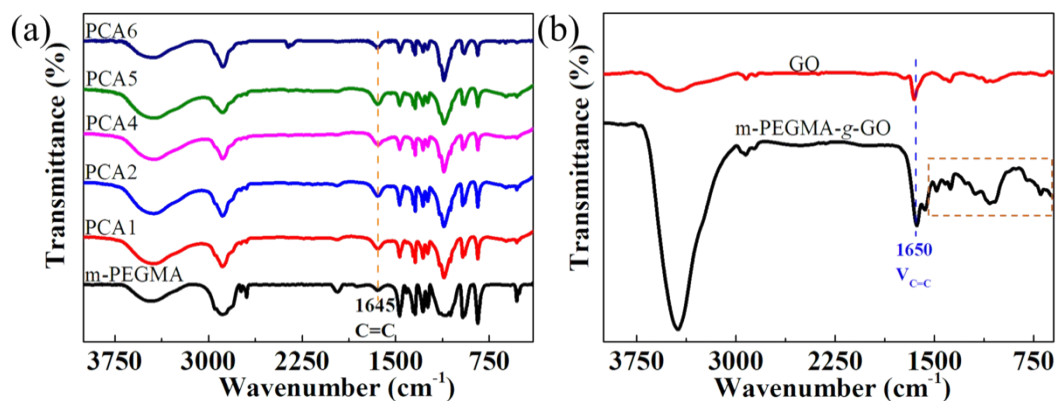


Fig. S1. (a) FT-IR spectra of m-PEGMA, PCA1, PCA2, PCA4, PCA5 and PCA6, (b) FT-IR spectra of GO and m-PEGMA-g-GO (Note that the m-PEGMA-g-GO comes from the PCA2 sample, which was exhaustively washed to remove the free m-PEGMA chains adsorbed on the surface of GO²).

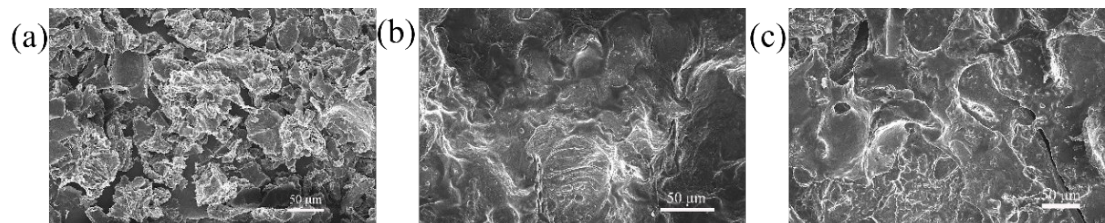


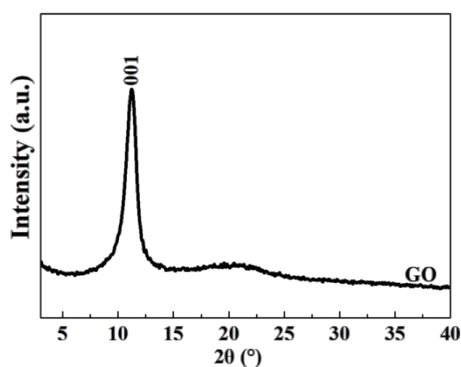
Fig. S2. SEM micrographs of (a) c-PCM, (b) PCA1, and (c) PCA5.

Table S2. Thermal stability of GO and PCAs from TGA analysis.

Specimen	GO (wt%) ^a	$T_5\%$ (°C)	W_{Re} (wt%)	GO (wt%) ^b
GO		67	35.09	
c-PCM	0.00	354	0.00	0.00
PCA1	0.50	359	0.68	1.94
PCA2	1.00	354	0.85	2.42
PCA3	1.50	360	0.97	2.76
PCA4	2.00	356	1.02	2.91
PCA5	3.00	354	1.62	4.62
PCA6	5.00	324	2.75	7.84

^a The loading of GO in the experimental section.

^b The actual loading of GO in the final specimen.

**Fig. S3.** XRD pattern of the raw GO.**Table S3.** X-ray diffraction data of PCAs.

Specimen	2θ (°)		$FWHM$		d_{101}	D_{101}	d_{021}	D_{021}
	101	021	101	021	(nm)	(nm)	(nm)	(nm)
c-PCM	19.180	23.340	0.470	0.709	0.462	16.951	0.381	11.314
PCA1	19.080	23.140	0.468	0.755	0.465	17.022	0.384	10.551
PCA2	19.240	23.440	0.566	0.794	0.461	14.078	0.379	10.099
PCA3	19.260	23.380	0.515	0.712	0.460	15.472	0.380	11.267
PCA4	19.180	23.420	0.534	0.707	0.462	14.920	0.380	11.348
PCA5	19.180	23.320	0.463	0.696	0.462	17.208	0.381	11.525
PCA6	19.260	23.380	0.484	0.706	0.460	16.463	0.380	11.363

Table S4. Thermal properties of different composite PCMs based on GO/RGO aerogel in the literatures.

Reference	PCMs	Heating rate (K/min)	ΔH_m (J/g)	χ (%)
[21]	Octadecanol (OA)	5	204	100.0
	RGO-2/OA (10% RGO)	5	166	90.4
	Stearic acid (SA)	5	185	100.0
	RGO-2/SA (10% RGO)	5	165	99.1
[30]	Paraffin	10	202.2	100.0
	MH-GP200 (3% RGO) ^a	10	201.5	102.7
[32]	Lauric acid (LA)	10	216.6	100.0
	LA (1.2% GOA) ^b	10	203.2	95.0
	LA (1.9% G ₂₅ -GO ₇₅ -CAs) ^c	10	207.9	97.8
	LA (2.0% G ₄₀ -GO ₆₀ -CAs) ^c	10	203.7	96.0
[26]	Tetradecanol (TD)	10	202.2	100.0
	TD/EGA-1 (5% EGA) ^d	10	191.8	100.8
	TD/EGA-2 (10% EGA) ^d	10	177.7	98.6
	TD/VGA-1 (5% VGA) ^e	10	190.1	100.0
	TD/VGA-2 (10% VGA) ^e	10	177.6	98.6
[54]	PPCM	10	86.8	100.0
	GPPCM (1.20% GA)	10	92.1	107.6
[13]	Paraffin wax (PW)	10	150.4	100.0
	PCM-C-MF-G-3 (3.65% RGO)	10	154.1	106.3
	PCM-C-MF-G3/6 (2.63% RGO)	10	155.3	106.0
	PCM-C-MF-G-3/12 (4.59% RGO)	10	154.1	107.4
	PCM-C-MF-G-3/18 (4.89% RGO)	10	155.5	108.7
This study	c-PCM (0.00% RGO)	10	154	100.0
	PCA2 (2.42% RGO)	10	170	113.1
	PCA3 (2.76% RGO)	10	177	118.2
	PCA4 (2.91% RGO)	10	176	117.7

^a MH-GP200: Graphene/paraffin aerogel prepared by a modified hydrothermal process.

^b GOA: Graphene oxide aerogel.

^c G_x-GO_y-CAs: Graphene/GO complex aerogels, in which *x* and *y* represented the weight ratio of graphene and GO, respectively.

^d EGA: Ethylenediamine-graphene aerogel.

^e VGA: vitamin C-graphene aerogel.

Table S5. DSC data of PCA3 before and after 100 thermal cycles.

Specimen	ΔH_m (J/g)	T_{mo} (°C)	T_{mp} (°C)	ΔH_c (J/g)	T_{co} (°C)	T_{cp} (°C)	ΔT (°C)
PCA3	177	47.1	58.7	176	35.2	27.3	11.9
PCA3-100 cycles	172	46.9	56.1	170	34.4	27.7	12.5

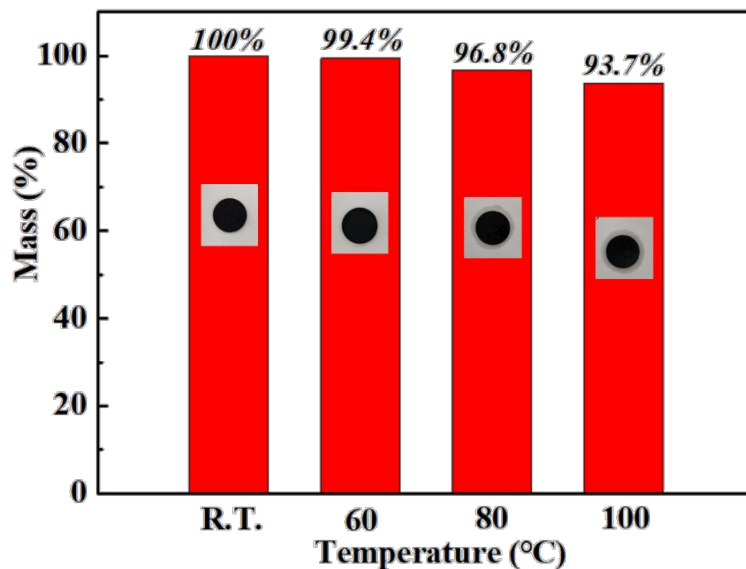


Fig. S4. Residual mass percentage of PCA3 sample after thermal treatment at different temperatures for 30 min (insert: photographs of PCA3 before and after thermal treatment).

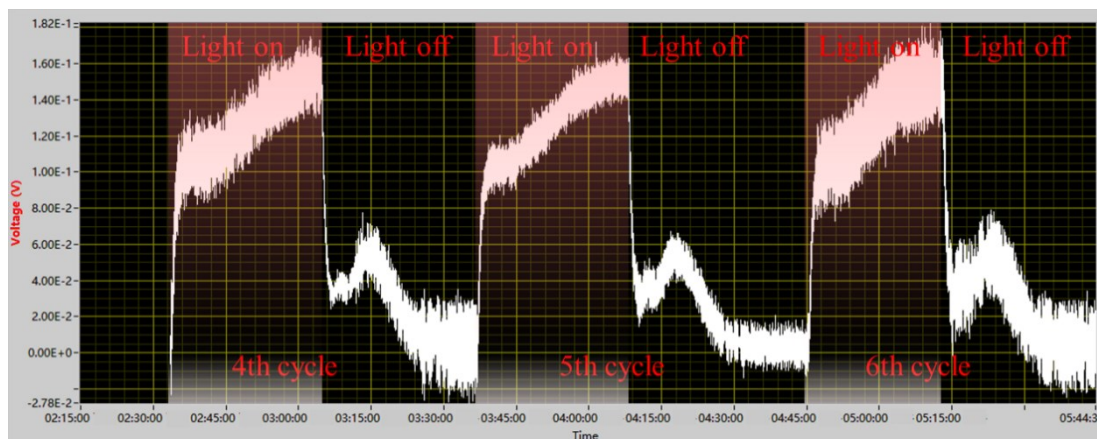


Fig. S5. Voltage output of PCA3-loaded TEG with and without solar light irradiation (200 mW/cm²).

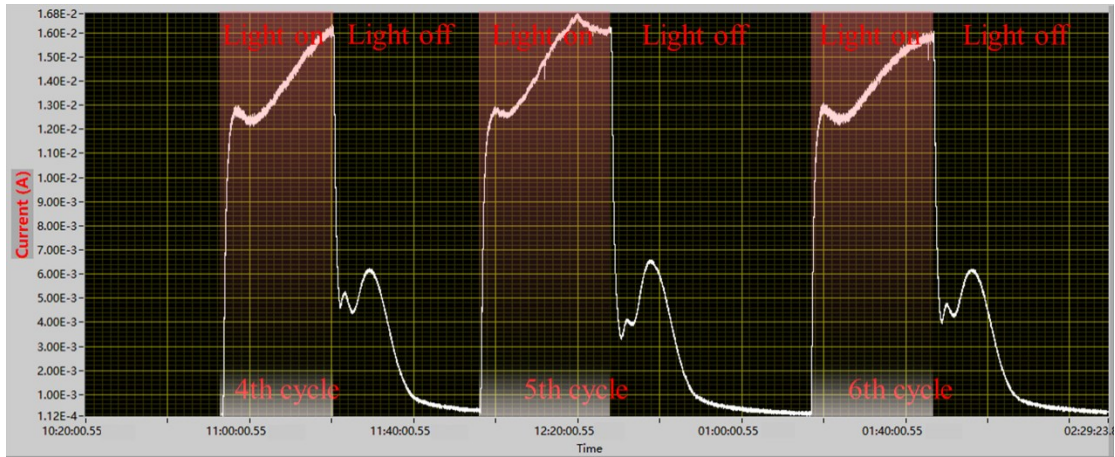


Fig. S6. Current output of PCA3-loaded TEG with and without solar light irradiation (200 mW/cm^2).

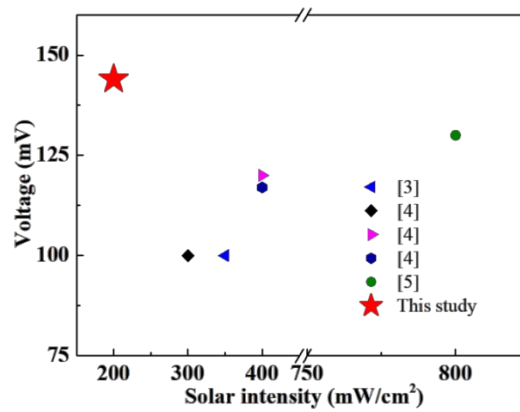


Fig. S7. Comparison of electric property (voltage output) of PCA3-loaded TEG in this study and previously reported in similar literatures that can be retrieved.

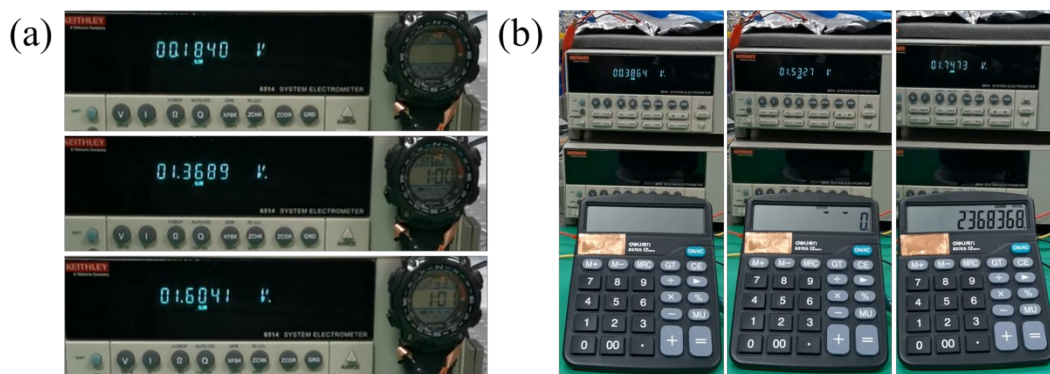


Fig. S8. Photos of powering several portable electronic gadgets by TEGs: (a) wrist watch, (b) commercial digital calculator.

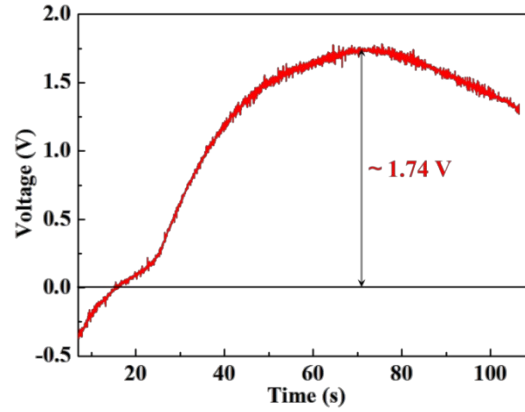


Fig. S9. Output voltage difference versus time curve of LEDs directly powered by PCA-loaded TEGs (TEG1+TEG2) and blank one.

Calculation of the thermal-to-electricity conversion maximum efficiency (η_{TEG}) of PCA3-loaded TEG and blank one

From **Fig. 4b** and **Fig. 4c** the hot side temperature of PCA3-loaded TEG and blank control sample can be obtained to be 70.8°C (343.95K) and 51.7°C (324.85K), respectively. Since the solar-thermal-electric conversion experiments was measured at room temperature, the cold side temperature of PCA3-loaded TEG and blank one is the same as the ambient temperature (about 27°C , 300.15K). In addition, the thermoelectric figure of merit (ZT) of the commercial TEG device used in this study is about 0.75~0.9. As is well known, most commercial thermoelectric materials at present typically give a limited ZT of about 0.8 at room temperature. Therefore, we take ZT value as 0.8 to calculate the η_{TEG} of PCA3-loaded TEG and blank one. After taking the above data to the formula (1) in the text, the η_{TEG} of T PCA3-loaded TEG and blank one can be obtained to be 9.34% and 5.79%, respectively. Compared to blank one, the η_{TEG} of PCA3-loaded TEG was increased by about 61.3%.

Calculation of the output power of PCA3-loaded TEG

According to the relevant literatures, there are two commonly used calculation methods for the output power of the TEG,⁶⁻⁸ and the two calculation equations are as follows:

$$P_{TE} = V_{TE} \times I_{TE} \quad (1)$$

where P_{TE} , V_{TE} and I_{TE} are the output power, voltage and current of the TEG, respectively.^{6,7}

$$P_{TE} = \frac{V_{open}^2}{R_{in}} \quad (2)$$

where V_{open} and R_{in} are the open circuit voltage and internal electrical resistance of the TEG, respectively. ⁸

Therefore, the output power of the TEG is calculated by Equation (1) to be about 2.13 mW. To verify the calculated value, the Equation (2) was also employed to estimate the output power of the TEG. The R_{in} of the TEG was measured using a multi-meter, and the measured value is 10.9 Ω , as shown in Fig. S10. Based on the Equation (2), the corresponding output power is about 1.90 mW.

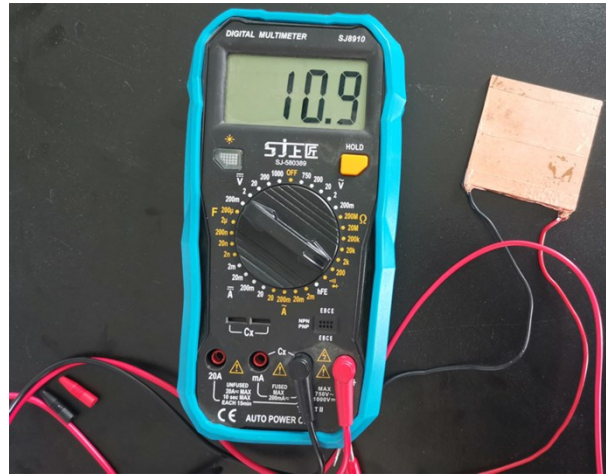


Fig. S10. Photograph of measuring R_{in} of the TEG

The calculated results of the two equations are nearly consistent, implying the reasonable estimated value in this manuscript. It should be noted that the output power value calculated by the Equation (2) is smaller than that from the Equation (1), which is due to the characteristic of TEG as current source.

Supporting Note 1

As is well known, ⁴ the output time of the steady-state current and voltage (i.e. current and voltage generated by TEG during phase change process) was shortened when increasing the simulated sunlight illumination intensity. However, when turning off the light illumination the output time of the steady-state current and voltage remained approximately constant because the shape and content of phase change working substrate in the PCAs were maintained during the whole process. More

importantly, even to increase the simulated sunlight intensity, the steady-state current and voltage with or without the light illumination are essentially unchanged.⁴ Hence, the influence of increasing the simulated sunlight intensity on the experimental results as follows: (1) the output time of the steady-state current and voltage was shortened; (2) after turning off the light illumination, however, the output and time of the steady-state current and voltage remained approximately constant in the whole process.

Therefore, in order to shorten the measuring time, the radiation intensity of 200 mW/cm² was applied in this manuscript. In fact, the measuring time has exceeded 5000 s with the radiation intensity of 200 mW/cm². In recent studies, the radiation intensity of more than 200 mW/cm², such as 250,⁹ 300,^{4, 10} 400,^{4, 11} 800^{4, 12} and 3000¹³ mW/cm², have been usually applied for the corresponding experimental measuring.

Reference

- [1] R.R. Cao, Y.Z. Wang, S. Chen, N. Han, H.H. Liu, X.X. Zhang, *ACS Appl. Mater. Inter.* 2019, **11**, 8982-8991.
- [2] R.R. Cao, H.H. Liu, S. Chen, D.F. Pei, J.L. Miao, X.X. Zhang, *Compos. Sci. Technol.* 2017, **149**, 262-268.
- [3] Y. Zhang, M.M. Umair, X. Jin, R.W. Lu, S.F. Zhang, B.T. Tang, *J. Mater. Chem. A* 2019, **7**, 8521-8526.
- [4] J. Yang, L.S. Tang, R.Y. Bao, L. Bai, Z.Y. Liu, W. Yang, B.H. Xie, M.B. Yang, *Chem. Eng. J.* 2017, **315**, 481-490.
- [5] J. Yang, L.S. Tang, R.Y. Bao, L. Bai, Z.Y. Liu, W. Yang, B.H. Xie, M.B. Yang, *J. Mater. Chem. A* 2016, **4**, 18841-18851.
- [6] J. Zhang, Y.M. Xuan, *Renew. Energ.* 2017, **113**, 1551-1558.
- [7] F. Rajaei, M.A.V. Rad, A. Kasaeian, O. Mahian, W.-M. Yan, *Energ. Convers. Manage.* 2020, **212**, 112780.
- [8] X.H. Luo, Q.G. Guo, Z.C. Tao, Y.J. Liang, Z.J. Liu, *Energ. Convers. Manage.* 2020, **208**, 112459.
- [9] X.S. Du, J.N. Xu, S. Deng, Z.L. Du, X. Cheng, H.B. Wang, *ACS Sustain. Chem. Eng.* 2019, **7**, 17682-17690.
- [10] Y. Zhang, G.G. Gurzadyan, M.M. Umair, W.T. Wang, R.W. Lu, S.F. Zhang, B.T.

Tang, *Chem. Eng. J.* 2018, **344**, 402-409.

[11] Q.H. Zhao, F.F. He, Q.P. Zhang, J.H. Fan, R. He, K. Zhang, H.J. Yan, W.B. Yang, *Sol. Energ. Mat. Sol. C.* 2019, **203**, 11204.

[12] J. Yang, L-S. Tang, R.-Y. Bao, B. Lu, Z.Y. Liu, B.-H. Xie, N.-B. Yang, W. Yang, *Sol. Energ. Mat. Sol. C.* 2018, **174**, 56-64.

[13] P. Tao, C. Chang, Z. Tong, H. Bao, C.Y. Song, J.B. Wu, W. Shang, T. Deng, *Energy Environ. Sci.* 2019, **12**, 1613-1621.